Power Loss Prediction and Precise Modeling of Magnetic Powder Components in DC–DC Power Converter Application

Alaa Hilal, *Student Member, IEEE*, Marie-Ange Raulet, Christian Martin, and Fabien Sixdenier

***Abstract*—In power electronics applications, magnetic components are often subjected to nonsinusoidal waveforms, variable frequencies, and dc bias conditions. These operating conditions generate different losses in the core compared to sinusoidal losses provided by manufacturers. In the conception and design stage, lack of precise losses diagnosis has unacceptable effects on system's efficiency, reliability, and power consumption. Since virtual prototyping is used to predict and improve system's behavior before realization, losses and behavior prediction of components is possible. Circuit simulators and their compatible components models are required. This paper is summarized by proposing nonlinear dynamic model of powdered material magnetic core for use in circuit simulators. It includes the material's nonlinear hysteresis behavior with accurate winding and core modeling. The magnetic component model is implemented in circuit simulation software "Simplorer" using VHDL–AMS modeling language. Waveforms and losses of a powder core inductor in a buck converter application are simulated and compared to measured ones. The model is validated for different ripple currents, different loads, and a wide frequency range. DC bias is taken into account in both continuous and discontinuous conduction modes.**

***Index Terms*—DC–DC converters, dynamic magnetic modeling, powder core, power losses, simulation.**

I. Introduction

POWER consumption and efficiency have always been of great concern in the development of power electronics systems. The increasing demand of low power, high efficiency devices [1], [2] forced designers to precisely analyze losses in each component constituting the system. In the design and analysis of systems in general, specifically power converters, virtual prototyping assure time, failure rate, and cost reduction [3]. Indeed modeling and simulation allow the prior knowledge of the power converter behavior using circuit simulators to optimize complex circuit prototypes. Individual components models exist and are associated together to form a complete converter model. Therefore, we are able to predict the whole system realistic behavior under variable operating conditions.

DC–DC power converters are a good example of such system where electrical power need to be "efficiently" stepped up or down from a dc voltage level to another. Passive components especially magnetic ones play a key role in power converters [4]; thus, behavior and loss analysis of these components is essential [5]–[7]. Since magnetic core losses calculation is a delicate subject, analytical equations as Steinmetz (SE) [8] fail to precisely calculate core losses due to limitation to sinusoidal excitation. Other improved formulas of SE like MSE [9], GSE [10], iGSE [11], and i2GSE [12] give better results but still limited due to their parameters variation as function of waveform, frequency and dc bias.

In this context, our work takes place by proposing a nonlinear dynamic model of magnetic components for use in circuit simulators. It includes the material nonlinear hysteresis and dynamic behaviors with accurate modeling of winding and core losses. The full model is described using VHDL–AMS [13] modeling language and implemented in the circuit simulator "Simplorer." It is tested for a powder core inductor in a widely used power convertor application, the buck converter, to ensure nonconventional excitation (square wave with dc bias). The model is validated for different ripple currents, different loads and a wide frequency range (10–100 kHz).

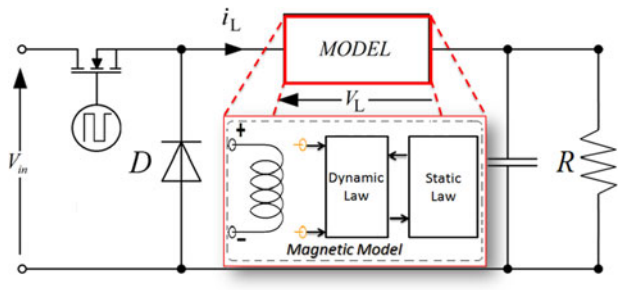

Fig. 1. Buck converter with the magnetic component structure.

II. Magnetic Model Concept

Inductors are components found in most power applications and converters. For each point of load application a specific design of these components is required. Considering a buck converter circuit Fig. 1, the magnetic component model would replace the inductor. In the interest of precision and in order to be adaptable for different types of magnetic materials, the inductor model must adopt a structural modeling approach. As a consequence the model consists of three major blocks: a winding allowing the coupling between electrical and magnetic domains

Manuscript received December 14, 2013; revised February 14, 2014 and March 24, 2014; accepted June 2, 2014. Date of publication June 13, 2014; date of current version November 3, 2014. Recommended for publication by Associate Editor C. R. Sullivan.

The authors are with the University of Lyon, University Lyon 1, CNRS UMR5005 AMPERE, Villeurbanne F69622, France (e-mail: alaa.hilal@univ-lyon1.fr; marie-ange.raulet@univ-lyon1.fr; christian.martin@univ-lyon1.fr; fabien.sixdenier@univ-lyon1.fr).

Color versions of one or more of the figures in this paper are available online at http://ieeexplore.ieee.org.

Digital Object Identifier 10.1109/TPEL.2014.2330952

using Ampere's and Faraday's laws, a static model to describe the static hysteresis behavior of the magnetic material and a dynamic model to add classical and excess losses in the core. VHDL–AMS language is chosen to describe each block behavior due to its multidomain modeling feature and since it is supported by several circuit simulators. Considering the operating frequency range, parasitic effects (such as interwinding capacitance) are negligible and not taken into account in the model.

Different static and dynamic models can be used to describe the behavior of magnetic material. The choice of the model depends on three main criteria: the material characteristics, the application and simulation factors like ease of implementation, accuracy and speed of simulation. Existing and well-known magnetic materials models such as Jiles–Atherton [14] and Preisach [15] are implemented in some circuit simulators. Nevertheless these material models are limited to static behavior where dynamic effects are either neglected or not well taken into account. Jiles–Atherton is a physical model requiring five parameters whose parameters identification requires a complex iterative process. Preisach is a statistical model requiring a weight function and large statistical data. However, both models do not apply for noncentered minor loops. The static and dynamic models chosen and their parameters identification are discussed in the following sections.

III. Magnetic Material Characterization and Modeling

The behavior of magnetic components depends mostly on magnetic properties and geometry of core material used. Each material has its specific hysteresis and dynamic behaviors. Hence, material characterization is mandatory to predict the appropriate static and dynamic models and their parameters.

A. Static Measurements and Modeling

Measurements are performed on a test transformer consisting of primary and secondary coils wound on a toroid powder core (Sendust Fe–Si–Al provided by TOHO ZINK) having a 4.6-mm inner diameter, a 10-mm outer diameter, and a 3.5-mm height. This material has a saturation induction of 0.7 T and a relative permeability $\mu_r = 100$. A sinusoidal current is applied to the primary winding, to create a magnetic field H and the flux density is calculated from the measured secondary voltage. Measurement results are shown in Fig. 2.

The magnetic material used has a very thin static hysteresis loop and thus a reversible behavior. To describe the static behavior of the material, a mathematical model based on a piecewise polynomial function of order *n* is used

$$B = \begin{cases} \mu_0 (H - H_b) + P(H_b), & \text{if} \quad H \geq +H_b \\ P(H), & \text{if} \quad |H| < H_b \\ \mu_0 (H + H_b) - P(H_b), & \text{if} \quad H \leq -H_b \end{cases} \tag{1}$$

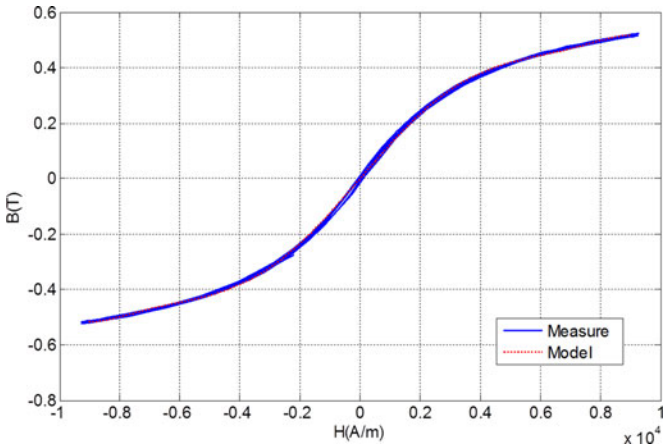

Fig. 2. Measured and simulated flux density as function of applied field at 1 kHz.

TABLE I
Static Parameters

P1	P3	P5	Hb(A/m)
1.3096e-04	–3.5058e-12	6.4788e-20	9000

where H_b is the field needed to reach saturation and P is a polynomial in $\mathbb{R}$ such that

$$P(\mathrm{X}) = \sum_{i=0}^{n} p_i X^i.$$

For this material, a polynomial of order 5 is sufficient and the even coefficients are almost zero due to the odd parity of the curve. This model is reversible and limited to materials with low coercive field [16]. The parameters of the static model given in Table I are identified from the static measurements using basic mathematical fitting. Accordance between static measurements and simulated B–H loop of the proposed model is shown in Fig. 2.

B. Dynamic Measurements and Modeling

Dynamic behavior is investigated by the proper choice of dynamic model. The model parameters extraction requires sinusoidal measurements at different induction levels at a single frequency. Dynamic measurements are performed on the same test transformer. Fig. 3 represents measured B–H loops under a 30-kHz sinusoidal applied flux density for three different induction levels.

The aim of these measurements is to study the dynamic losses arising in the material due to relatively high-frequency applied flux density as well as the influence of its level. The B–H loop enlargement with the induction increase is shown.

The dynamic model is based on the principle of separation of losses into static and dynamic contributions, as well as Bertotti's theory [17] assuming that the dynamic loss is the sum of both classical and excess losses. The total magnetic field is the sum of static field due to hysteresis and dynamic fields due to eddy

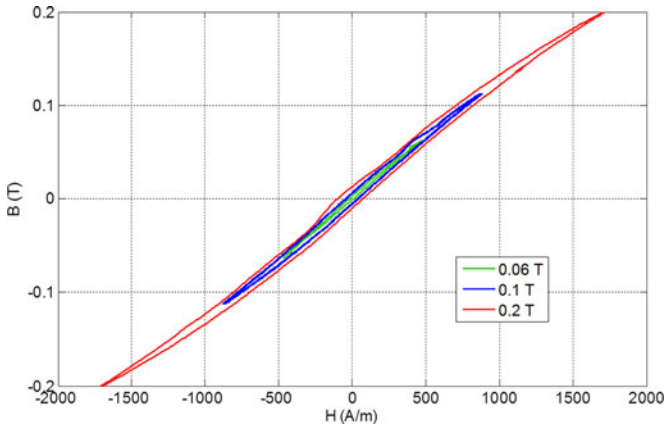

Fig. 3. Measured flux density as function of applied field at $f = 30$ kHz for different induction levels.

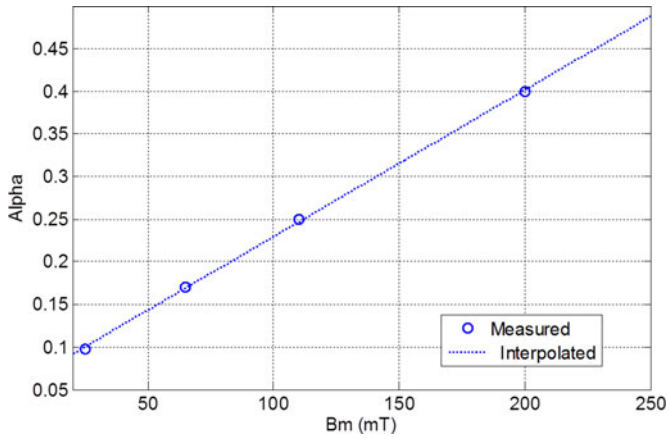

Fig. 4. Parameter α variation as function of maximum flux density level.

currents and wall motion effects (2).

$$H_{\text{total}}(t) = H_s(B(t)) + \gamma \cdot \frac{dB(t)}{dt} + \alpha \cdot \delta \cdot \left|\frac{dB(t)}{dt}\right|^{0.5} \quad (2)$$

where γ, α, and δ represent the eddy current, the wall motion, and the sign coefficients, respectively, presented in (3). γ depends on the material's conductivity σ_p and particle average size of powder core r_p. It is derived from the general equation proposed in [18]. α is a function of the characteristic field V_0, a dimensionless coefficient G, and the magnetic cross section S as proposed by Bertotti

$$\gamma = \frac{\sigma_p r_p^2}{8}, \quad \alpha = \sqrt{\sigma_p G V_0 S}, \quad \delta = \text{sign}\left(\frac{dB}{dt}\right). \quad (3)$$

The resistivity of the used powder core (sendust) is about 100 $\mu\Omega$·cm and the average particle size is found to be 70 μm. Since γ depends only on these two core characteristics, it is directly calculated (1.53×10^{-4}). The other parameter α is extracted from mathematical fitting of (2) to the measured B–H loop at 30 kHz, i.e., it is calculated in order to have the same measured and simulated B–H loops. Tracing the wall motion parameter α variation as a function of induction level we find a linear variation as shown in Fig. 4. Interpolation of α is inserted in the model to estimate iron losses at different flux density levels.

IV. Buck Converter Application

In many power applications, magnetic materials are excited with nonsinusoidal waveforms. This induces different losses compared to those provided by manufacturers based on sinusoidal flux density [19]. DC bias has also a significant effect on losses [20]. In buck converter, a PWM voltage is applied on the inductor and a dc bias depending on the load exists. This would create a noncentered minor hysteresis loop. As a consequence core loss prediction becomes complex, and precise magnetic modeling is required.

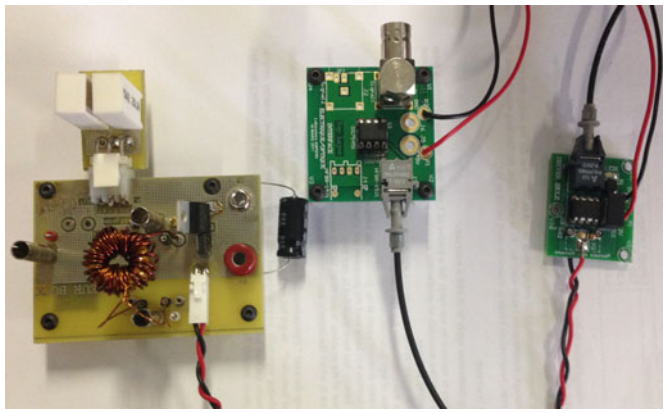

Fig. 5. Buck converter measurement circuit.

A. Buck Circuit and Losses Measurements

In order to investigate magnetic component behavior in power applications, a 40-W buck converter shown in Fig. 5 is realized. The circuit design allows variable voltage, frequency and load. Inductor used in the circuit is the same powder core previously characterized with 30 turns copper wire.

To measure precisely magnetic losses, a small shunt (200 mΩ) is added in series with the inductor and ten secondary turns are wound to the same core. The shunt allows precise current measurements, while open secondary side allows voltage measurement excluding coil losses. Both measurements are performed by a 1.5–6 GHz bandwidth, 40 GS/s LECROY oscilloscope. Knowing the primary current and secondary voltage, iron losses are calculated using

$$P = \frac{1}{T}\int_0^T \frac{N_1}{N_2} v_2(t) \cdot i_1(t) \cdot dt. \quad (4)$$

Concerning copper losses, they are calculated using (5) where the total power dissipated in the windings is the sum of dc and ac losses. I_{DC} and R_{DC} are the dc current and resistance, respectively. R_{DC} is derived from conductor resistivity and dimensions. R_{AC} is the ac resistance due to skin and proximity effects that increase with frequency. I_n is the current's nth harmonic.

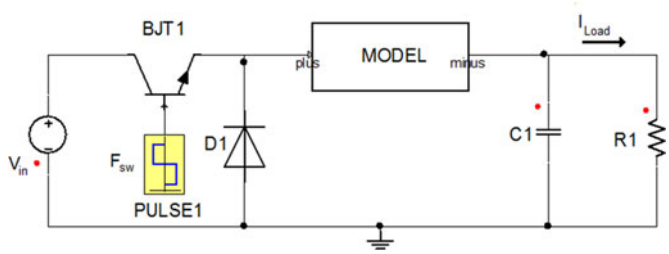

Fig. 6. Buck converter simulation circuit.

The ac resistance can be determined either by calculation according to [21], or by measurement using a coreless winding and an impedance analyzer (we used the Agilent 4294A). In both cases, the ac copper losses are negligible, not more than 1% of total winding losses. This is due to low ac current in the buck application and to low ac resistance increase for the operating frequency range (up to 100 kHz). Hence, the copper losses can be limited to dc loss only. The winding loss for the used 30 turns copper wire is found to be 39 mW at a dc current of 1 A

$$P_w = P_{\mathrm{DC}} + P_{\mathrm{AC}} = R_{\mathrm{DC}} I_{\mathrm{DC}}^2 + \sum_n R_{\mathrm{AC}n} I_n^2 \approx R_{\mathrm{DC}} I_{\mathrm{DC}}^2. \tag{5}$$

B. Circuit Simulation and Losses Prediction

To validate our model a circuit identical to the buck circuit used for measurements is simulated in Simplorer as shown in Fig. 6. The model replaced the inductor including both static and dynamic models (blocks) plus core dimensions. Winding resistance and number of turns are inserted to the winding block in the model. Each of these blocks is a separate VHDL–AMS "Subsheet" (containing the code). An example of the Bertotti's block code is presented below. Comparison between measured and simulated waveforms and losses is presented in the next section.

```
LIBRARY ieee;
LIBRARY std;
LIBRARY basic_vhdlams;
– – – – – – –VHDLAMS MODEL BERTOTTI – – – – – –
–
USE basic_vhdlams.ALL;
USE std.ALL;
USE ieee.ALL;
– – – – –ENTITY DECLARATION BERTOTTI – – – – –
–
ENTIT DYN IS
      generic(
            s : real := 0.000009; – – Effective
      Area of Core
            l : real := 0.023); – – Effective
      Length of Core
      port( TERMINAL n1, n2 : MAGNETIC;
                  QUANTITY B : out real;
                  QUANTITY Hs : in real);
END ENTITY DYN;
```

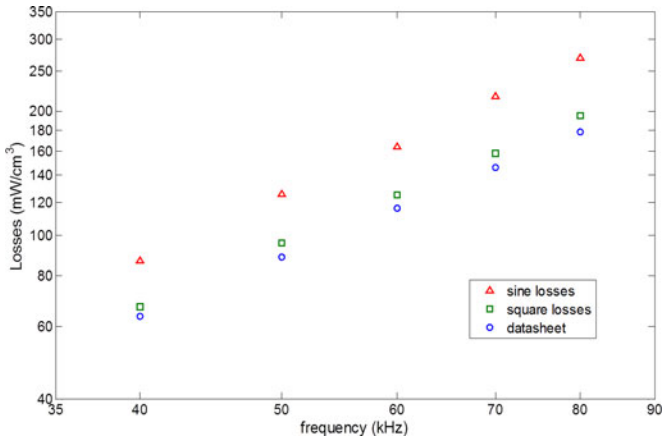

Fig. 7. Measured sine and square losses and datasheet losses at $B = 100$ mT.

```
– – ARCHITECTURE DECLARATION arch_BERTOTTI – –
ARCHITECTURE arch_DYN OF DYN IS
      QUANTITY MV ACROSS flux THROUGH n1 TO n2;
– – – – – – – – – DYNAMIC PARAMETERS – – – – – – –
–
      CONSTANT gamma : real := 1.531e – 4;
      – – dynamic parameter 1
      CONSTANT alpha : real := 13.30e – 2;
      – – dynamic parameter 2
      QUANTITY D : real;
      QUANTITY Hd : real;
      QUANTITY delta : real;
– – – – – – – – – – – BEHAVOIUR – – – – – – – – –
BEGIN
      B == flux/s;
      Hd == MV/l;
      D == B'dot;
      if Hs'dot > 0.0 use delta == 1.0;
            else delta == –1.0;
            end use;
Hd == Hs + gamma*D + alpha*delta*(delta*D)**0.5;
END ARCHITECTURE arch_DYN;
– – – – – – END VHDLAMS MODEL BERTOTTI – – – – –
```

C. Results and Discussion

As mentioned earlier, losses under sinusoidal and nonsinusoidal excitation are not the same. To demonstrate that, Fig. 7 presents losses measured in the powder core under sinusoidal and square voltage excitations at 50% duty cycle (Sections III-B and IV-A, respectively). These measurements are carried out under a constant level magnetic flux density (100 mT) and for a frequency range between 40 and 100 kHz. Then datasheet losses calculated using Steinmetz equation and parameters both provided by the constructor [22].

The data sheet losses calculated using the square waveform parameters provided by the manufacturer correspond to the measured ones. We can notice that these square losses at 50% duty cycle are lower than sine losses. However, for extreme duty cycles, square losses become higher than sine losses. This is

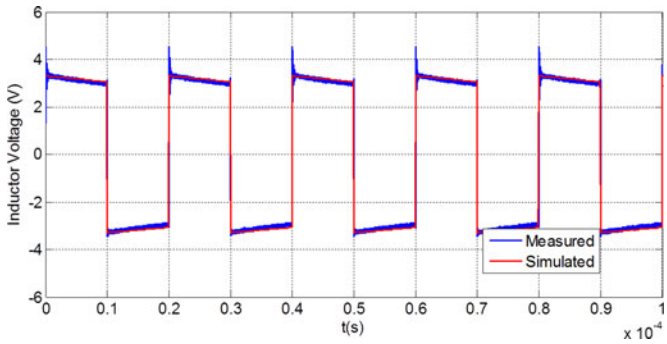

Fig. 8. Measured and simulated inductor voltage at $f = 50$ kHz.

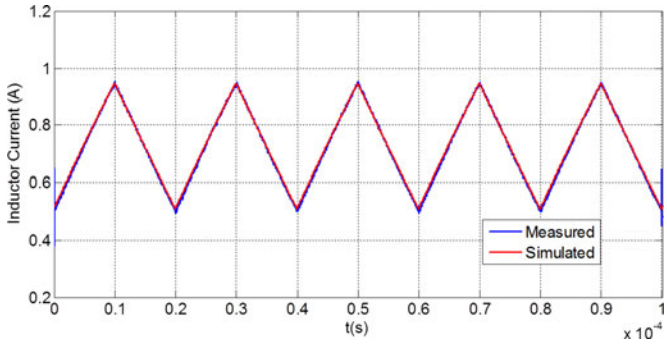

Fig. 9. Measured and simulated inductor current at $f = 50$ kHz.

due to the fact that losses are function of magnetic induction time derivative. Using sine losses for materials excited by other waveforms or vice versa is quite a drawback for systems design, regarding efficiency and power consumption.

In view of all previous circumstances, a complete magnetic model has many advantages. For instance, the exact inductor voltage and current of both continuous and discontinuous conduction modes are available from circuit simulation. Results are presented in Figs. 8 and 9. Measured and simulated waveforms are in good agreement.

Furthermore simulated iron losses (buck in continuous conduction mode) for different induction levels are compared to measured ones in the 40 to 100 kHz frequency range. Results are shown in Fig. 10. We note that only a single dynamic parameter "α" has to be identified from sinusoidal measurements. Experiments confirm model's loss prediction accuracy with a maximum error of 3%.

To study dc bias effects on magnetic losses, a set of five load circuits, consisting of ceramic cased power resistors, are used to vary dc current in the buck circuit. These resistive loads having values of 2, 3, 4.4, 5, and 6 Ω are connected and iron losses are measured simultaneously. Measurements done under fixed 5 V input voltage and 25 kHz frequency are shown in Fig. 11.

On the one hand, for dc currents higher than 600 mA the inductor is in continuous current mode. The dc bias effect here is insignificant due to very low hysteresis losses in the powder core material and a slight change in the dc current. This effect is explained in Fig. 12; applying the same ΔB of 0.2 T at

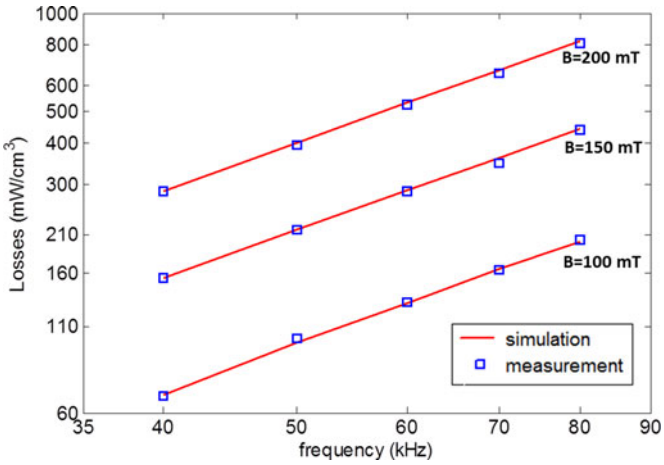

Fig. 10. Measured and simulated core losses.

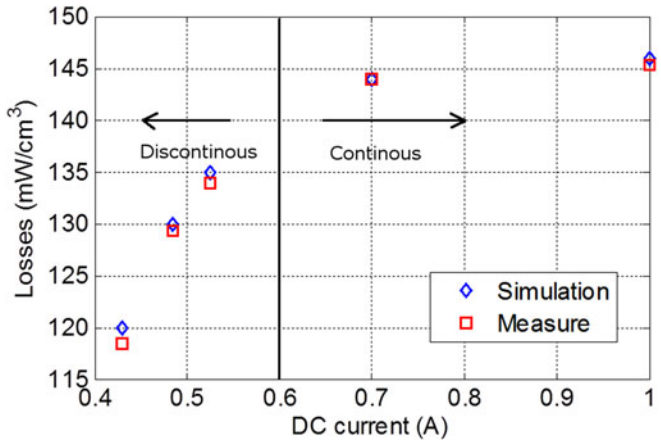

Fig. 11. Simulated and measured core losses under variable load currents.

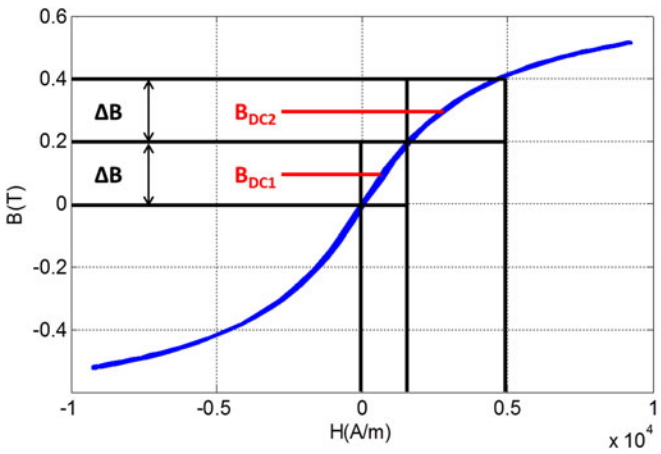

Fig. 12. Effect of variable dc bias.

two different dc levels B_{DC1} and B_{DC2} give two different ΔH values, and then two minor hysteresis loops with different areas.

On the other hand, for dc currents lower than 600 mA the inductor operates in discontinuous conduction mode. In this case, we still have the same flux density derivative (as voltage

and frequency are the same) but with smaller ΔB and ΔH corresponding to the smaller ripple current ΔI (due to discontinuity). As a result, we generate smaller minor *B–H* loops and thus lower losses. We can observe the losses decrease with dc current decrease.

Finally, our model is a real-time approach while all analytical formulas are posteriori approaches. Here lies the importance of magnetic components modeling.

V. Conclusion and Perspectives

In this paper, the behavior of a power inductor in a widely used power converter topology is studied. Development of a magnetic component model for use in circuit simulation is presented. Simulations of a buck converter including the proposed model are compared to measurements performed on a converter circuit of variable voltage, switching frequency and load. The magnetic component model allows precise prediction of core and winding losses. Simulated inductor current and voltage correspond to measured ones. Model's parameters are extracted from magnetic material characterization under sinusoidal excitation. Experiments confirm model's loss prediction accuracy with a maximum error of 3% for nonsinusoidal waveforms. DC bias is taken into account. Both continuous and discontinuous conduction modes are studied. Results are in good agreement for different induction levels and a wide frequency range. The model is limited to negligible skin effects conditions, since magnetic diffusion is not taken into account. Relaxation losses [12] are not fully taken into account either. Both effects will be studied in future work by implementing more complex static (relaxation effect) and dynamic (diffusion effect) material's laws. Simulation of other circuits, including thermal effects is also of our interest for future work.

References

[1] R. Priewasser, M. Agostinelli, C. Unterrieder, S. Marsili, and M. Huemer, "Modeling, control, and implementation of DC–DC converters for variable frequency operation," *IEEE Trans. Power. Electron.*, vol. 29, no. 1, pp. 287–301, Jan. 2014.

[2] O. Sheng-Yuan and H. Ho-Pu, "Analysis and design of a novel single-stage switching power supply with half-bridge topology," *IEEE Trans. Power. Electron.*, vol. 26, no. 11, pp. 3230–3241, Nov. 2011.

[3] J. Popovic-Gerber, J. A. Oliver, N. Cordero, T. Harder, J. A. Cobos, M. Hayes, S. C. O'Mathuna, and E. Prem, "Power electronics enabling efficient energy usage: Energy savings potential and technological challenges," *IEEE Trans. Power Electron.*, vol. 27, no. 5, pp. 2338–2353, May 2012.

[4] N. A. Spaldin, *Magnetic Materials: Fundamentals and Applications*. Cambridge, U.K.: Cambridge Univ. Press, 2010.

[5] P. R. Wilson, J. Neil Ross, and A. D. Brown, "Simulation of magnetic component models in electric circuits including dynamic thermal effects," *IEEE Trans. Power Electron.*, vol. 17, no. 1, pp. 55–65, Jan. 2002.

[6] W. Chandrasena, P. McLaren, U. Annakkage, R. Jayasinghe, D. Muthumuni, and E. Dirks, "Simulation of hysteresis and eddy current effects in a power transformer," *Elec. Power Syst. Res.*, vol. 76, pp. 634–641, May 2006.

[7] G. Gruosso and A. Brambilla, "Magnetic core model for circuit simulations including losses and hysteresis," *Int. J. Numerical Modeling*, vol. 21, pp. 309–334, 2008.

[8] C. P. Steinmetz, "On the law of hysteresis," *Proc. IEEE*, vol. 72, no. 2, pp. 197–221, Feb. 1984.

[9] J. Reinert, A. Brockmeyer, and R. De Doncker, "Calculation of losses in ferro- and ferrimagnetic materials based on the modified steinmetz equation," *IEEE Trans. Ind. Appl.*, vol. 37, no. 4, pp. 1055–1061, Jul./Aug. 2001.

[10] J. Li, T. Abdallah, and C. R. Sullivan, "Improved calculation of core loss with nonsinusoidal waveforms," in *Proc. IEEE Annu. Meet. Ind. Appl. Soc.*, 2001, pp. 2203–2210.

[11] K. Venkatachalam, C. R. Sullivan, T. Abdallah, and H. Tacca, "Accurate prediction of ferrite core loss with non-sinusoidal waveforms using only Steinmetz parameters," in *Proc. IEEE Workshop Comput. Power Electron.*, 2002, pp. 36–41.

[12] J. Muhlethaler, J. Biela, J. W. Kolar, and A. Ecklebe, "Improved core-loss calculation for magnetic components employed in power electronic systems," *IEEE Trans. Power. Electron.*, vol. 27, no. 2, pp. 964–973, Feb. 2012.

[13] S. Cooper and M. Graphics, "An introduction to the VHDL-AMS modeling language," *Denver Chapter IEEE Power. Electron. Soc.*, Nov. 2007.

[14] D. C. Jiles and D. L. Atherton, "Theory of ferromagnetic hysteresis," *J. Mag. Mag. Mater.*, vol. 61, pp. 48–60, 1986.

[15] A. Courtay, *The Preisach Model*, Analogy, Inc., Austin, TX, USA, 1999.

[16] T. Chailloux, M. A. Raulet, C. Martin, C. Joubert, F. Sixdenier, and L. Morel, "Magnetic behavior representation taking into account the temperature of a magnetic nanocrystalline material," *IEEE Trans. Magn.*, vol. 48, no. 2, pp. 455–458, Feb. 2012.

[17] G. Bertotti, "General properties of power losses in soft ferromagnetic materials," *IEEE Trans. Mag.*, vol. 24, no. 1, pp. 621–630, Jan. 1988.

[18] H. Skarrie, "Design of powder core inductors," Licentiate, Dept. Indust. Elect. Eng Automat., Lund Univ., Lund, Sweden, 2001.

[19] A. Boglietti, A. Cavagnino, M. Lazzari, and M. Pastorelli, "Predicting iron losses in soft magnetic materials with arbitrary voltage supply: An engineering approach," *IEEE Trans. Magn.*, vol. 39, no. 2, pp. 981–989, Mar. 2003.

[20] C. A. Baguley, B. Carsten, and U. K. Madawala, "The effect of DC bias conditions on ferrite core losses," *IEEE Trans. Magn.*, vol. 44, no. 2, pp. 246–252, Feb. 2008.

[21] P. L. Dowell, "Effects of eddy currents in transformer windings," *Proc. Inst. Elect. Eng.*, vol. 113, no. 8, pp. 1387–1394, Aug. 1966.

[22] TOHO ZINC, "Soft magnetic materials of TOHO ZINC."

Alaa Hilal (S'13) was born in Btekhnay, Lebanon, in 1987. He received the bachelor's and M.Sc. degrees in electronics and embedded systems from Lebanese University, Beirut, Lebanon, in 2009 and 2011, respectively. He is currently working toward the Ph.D. degree in electrical engineering at the University of Claude Bernard Lyon 1, Lyon, France.

In 2011, he got an internship at the National Institute of Applied Sciences of Lyon for Scientific and Technological Research for his M.Sc. His research interests include magnetic components modeling for power electronics applications, mainly dc–dc converters, circuit simulators and programing languages.

Marie-Ange Raulet received the electrical engineering degree from the Institut National Polytechnique (INP) de Toulouse, Toulouse, France, in 1986, and Ph.D. degree in electrical engineering from the same institute in 1990.

She is a Full-Time Lecturer at the University Claude Bernard Lyon 1 and a Researcher at the Ampere Laboratory. Her research interests include the elaboration of accurate magnetic laws and their implementation in field calculations.

Christian Martin was born in 1979. He received the Engineer degree from the Institut National Polytechnique de Grenoble, Grenoble, France, in 2002, and the M.Sc. and Ph.D. degrees from the Joseph Fourier University, Grenoble, in 2002 and 2005, respectively.

He is currently an Associate Professor at the University of Lyon and leads his research with the AMPERE Laboratory. His research interests include magnetic material characterization and modeling, design, and integration of magnetic component for power electronics systems.

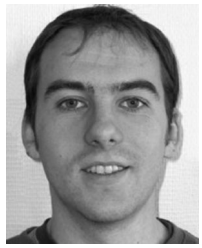

Fabien Sixdenier received the electrical engineering degree from the University of Claude Bernard Lyon 1, Lyon, France, in 2002, and the Ph.D. degree from the same university in 2005.

Since 2006, he has been a Full-Time Lecturer at the University Claude Bernard Lyon 1 and a Researcher at the Ampere Laboratory. His research interests include magnetic materials and their applications, especially accurate magnetic material modeling in actuators.